

### MECHANICAL PROPERTIES OF METASTABLE MATERIALS CONTAINING STRONG DISORDER

# Remarks on the Notch Sensitivity of Bulk Metallic Glasses

YANCHUN ZHAO (p)1,2,3,4 and YANFEI GAO (p)3,5

1.—State Key Laboratory of Advanced Processing and Recycling of Non-Ferrous Metals, Lanzhou University of Technology, Lanzhou 730050, People's Republic of China. 2.—College of Materials Science and Technology, Lanzhou University of Technology, Lanzhou 730050, People's Republic of China. 3.—Department of Materials Science and Engineering, University of Tennessee, Knoxville, TN 37996, USA. 4.—e-mail: yanchun\_zhao@163.com. 5.—e-mail: ygao7@utk.edu

Since the degree of stress triaxiality can be easily manipulated in notched samples, tests on them can provide crucial information to verify various constitutive models of bulk metallic glasses (BMGs). Oftentimes, notched samples exhibit enhanced ductility, but their strength can be reduced or improved, or even be insensitive to, the notch geometric parameters. Based on a comparison of notch studies on conventional metallic materials (that exhibit cavitation-controlled failure) and composites (that exhibit crack bridging), as well as by assembling many recent notch studies on BMGs, this review assesses the following key factors: the role of stress triaxiality in the atomistic processes for free volume evolution, the competition between and synergy of shear banding and cavitation failure, and the geometric arrangements of shear bands that delay shear or cavitation failure. Difficulties that prevent unified predictions are also explained.

### INTRODUCTION

In macroscopic mechanical tests such as those based on tension and bending, bulk metallic glasses (BMGs) exhibit strain localization into narrow bands, called shear bands since they often align with the principal shear stress directions, in spite of small deviations. Although a consensus on the detailed atomistic processes for shear band initiation and growth remains elusive, a mechanistic interpretation of such strain localizations can be obtained from the instability of constitutive relationships in the classic Hill–Hutchinson–Rice framework. 1,2 Consequently, constitutive modeling provides an indispensable link between structural dynamic studies on the atomistic scale and experimental observations using a wide range of mechanical testing methods. One critical assessment along this line is focused on mechanistic predictions using various candidate constitutive laws, e.g., for the conditions for the onset of shear bands, shear band arrangement, their temperature and strain-rate dependence, and their evolution into failure; For example, the deformation of conventional metals and alloys is governed by dislocation slips and various interaction mechanisms. When the dislocation density in face-centered cubic (FCC) crystals is

sufficiently large, their collective behavior can be described by the Schmid law, whose validity requires testing using atomistic modeling. For a polycrystalline metal, by averaging the Schmid-type crystal plasticity over individual grains, the macroscopic deformation now behaves as the Mises plasticity, whereas the Taylor factor connects the Schmid and Mises models. While individual dislocation slip lines can be regarded as the instability from the Schmid-type constitutive law because of the corners on the yield surface, the Mises plasticity is very resistant to any strain localization, unless there are additional mechanisms for strain softening or pressure sensitivity. Casting this Schmid-Mises relationship into BMGs, it is noted that the macroscopic strain localization exhibits characteristics resembling those of pressure-sensitive materials, as well as the transient heating in shear bands. For the former, the shear band directions depend on the degree of pressure sensitivity (e.g., the friction coefficient in the Mohr–Coulomb model) and the flow nonnormality. Thus, mechanical tests with various degrees of stress triaxiality can be conducted to test various ways in which pressure can be incorporated into the constitutive law. One method often applied along this line is notch testing, as discussed herein. For the latter, the BMG

878 Zhao and Gao

community tends to agree on the understanding that the thermal effect is an after-effect of shear band initiation, although its role in shear band propagation remains under debate.<sup>3</sup> Nevertheless, this review only focuses on the effect of various stress states as obtained from notch testing.

Before we discuss the experimental observations of notch effects in BMGs, it is advisable to start with a brief review of notch sensitivity in fracture mechanics analysis, with a focus on the crackbridging concept in composites 4,5 and the material failure model in conventional metallic materials. In the quintessential problem shown in Fig. 1, adapted from Bao and Suo, 4 the crack is represented by a cohesive interface model that relates the traction and interfacial separation through a micromechanically derived or phenomenological constitutive law, characterized by a reference stress  $\sigma_0$  and a reference separation  $\delta_0$ . From both dimensional analysis and numerical simulations, the crack-bridging zone is found to scale as  $E\delta_0/\sigma_0$ , where E is the Young's modulus. Therefore, the maximum value of the applied load,  $\sigma_{\infty}^{\max}$ , depends on the ratio of this crack-bridging zone and the notch root radius,

$$\Lambda = \frac{E\delta_0}{\sigma_0 a}.\tag{1}$$

When  $\Lambda \to 0$ , the crack-bridging zone is very small compared with the crack size or other geometric features, so that the failure is governed by linear elastic fracture mechanics (LEFM) and  $\sigma_{\infty}^{\max}/\sigma_0$  is merely the inverse of the stress concentration factor at the notch root (about 1/3 when  $L/W \to 1$ ). This is the limit of small-scale bridging (SSB). On the other limit, a large  $\Lambda$  indicates large-scale bridging (LSB) behavior, and the failure is then governed by the strength of the cohesive interface, given by  $\sigma_{\infty}^{\max}/\sigma_0 = L/W$ . The crack-bridging concept therefore nicely unifies the LEFM analysis and the strength analysis, as shown in the flowchart in Fig. 2 (also modified from Ref. 4), which finds a wide range of applications in composite research,

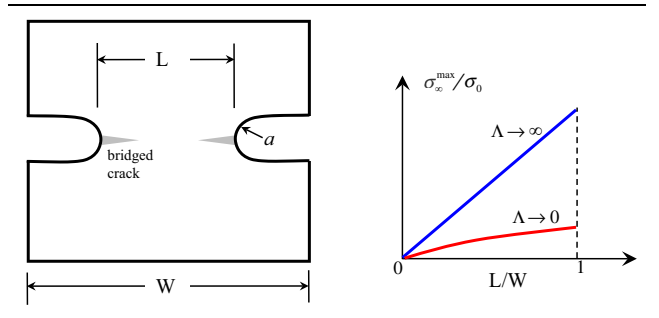


Fig. 1. Notch sensitivity in composites as modeled by the bridged crack (modified from Bao and Suo<sup>4</sup>). Geometric illustration of the double-edge notched sample, where the ratio of the extent of crack-bridging zone to the notch root radius dictates the small-scale bridging (SSB, low  $\Lambda$ ) to large-scale bridging (LSB, large  $\Lambda$ ) transition. The dimensionless parameter is  $\Lambda = E \delta_0/(a\sigma_0)$ .

particularly for the synergistic increase of strength and toughness through microstructural design. It is also worth noting that the LSB (i.e., strengthgoverned) limit corresponds to the flaw tolerance in biomimetics.<sup>8</sup>

In conventional metallic materials, the crack tip is shielded by plastic deformation, and similarly we can find small-scale yielding (SSY) and large-scale yielding (LSY) when comparing the plastic zone size to the crack size or other feature sizes that limit the K-annulus. No failure can be predicted from plastic zone analysis, so a micromechanical failure model must be embedded along the crack path, as shown in Fig. 3. In the classic Gurson–Tvergaard–Needleman (GTN) model, <sup>6,7</sup> the yield surface is defined by

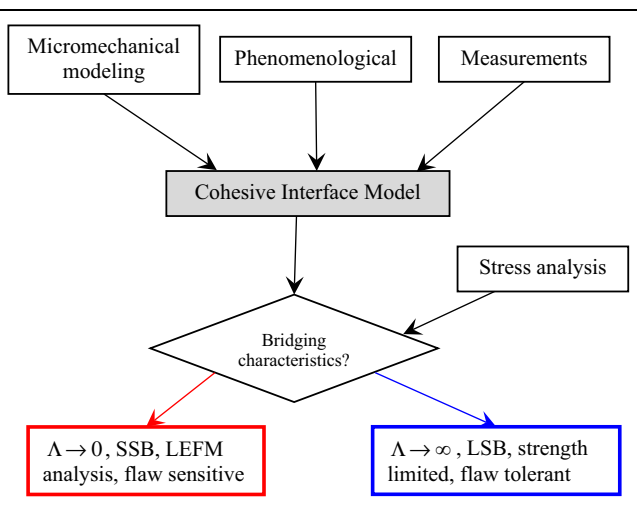


Fig. 2. Small-scale bridging (SSB) and large-scale bridging (LSB) are dictated by the cohesive interface model and the stress analysis. Notch- and flaw-sensitive conditions correspond to SSB, while flow-tolerant behavior corresponds to LSB. This schematic (modified from Bao and Suo<sup>4</sup>) applies to composites and biomimetics.

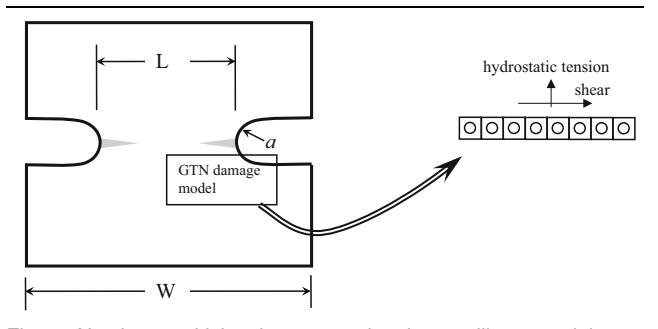


Fig. 3. Notch sensitivity in conventional metallic materials as modeled by the Gurson–Tvergaard–Needleman (GTN) model. The void-based GTN model has no length scale, so the extent of damage zone depends on the initial void distribution and the extent of plastic zone as governed by the boundary-value problem.

$$\Phi = \left(rac{\sigma_{
m e}}{\sigma_{
m Y}}
ight)^2 + 2q_1f^*\cosh\!\left(rac{3q_2\sigma_{
m m}}{2\sigma_{
m Y}}
ight) - 1 - \left(q_1f^*
ight)^2, ~~(2)$$

where  $\sigma_e$ ,  $\sigma_m$ , and  $\sigma_Y$  are the Mises stress, mean stress, and yield strength of the nonporous solid, respectively, and the parameter  $f^*$  is related to the porosity f by

$$f^* = \begin{cases} f, & f < f_c \\ f_c + \frac{(1/q_1 - f_c)(f - f_c)}{f_f - f_c}, & f \ge f_c \end{cases}$$
(3)

with fitting parameters  $f_c$ ,  $f_f$ ,  $q_1$ , and  $q_2$ . The cavities nucleate and grow according to

$$\dot{f} = (1 - f)\dot{\varepsilon}_{kk}^p + \dot{f}_{nucl},\tag{4}$$

with the plastic strain-rate tensor  $\dot{\varepsilon}_{ii}^p$ . As Eq. 4 is dictated by the volumetric plastic deformation, the extent of the damage zone depends on the way in which the stress triaxiality is modeled in Eq. 2 e.g., a number of variant GTN models are given in Ref. 9, and also the stress state ahead of the cracks, holes, notches, or more general boundary-value problems. Along the latter line of thought, Needleman and Tvergaard<sup>10</sup> conducted extensive finite element simulations of the failure process in notched round bars. As shown schematically in Fig. 4, the fracture strain decreases dramatically with increase of the stress triaxiality, defined as  $T = \sigma_{\rm m}/\sigma_{\rm e}$ , obviously due to the role of mean stress in enlarging the voids in the GTN model. More interestingly, their results can be characterized by the extent of the damage zone; in the limit of large-scale damage (LSD), the fracture strain will be considerably larger than that of small-scale damage (SSD). Note that the GTN model has no length scale, so the extent of the damage zone depends on the notch geometry and the ratio  $\sigma_{\infty}/\sigma_{Y}$ , but the fracture energy shows mesh size dependence.

These prior understandings in Figs. 1, 2, 3 and 4 lay the foundation to understand the notch effects in BMGs. Loosely speaking, the shear-band-induced

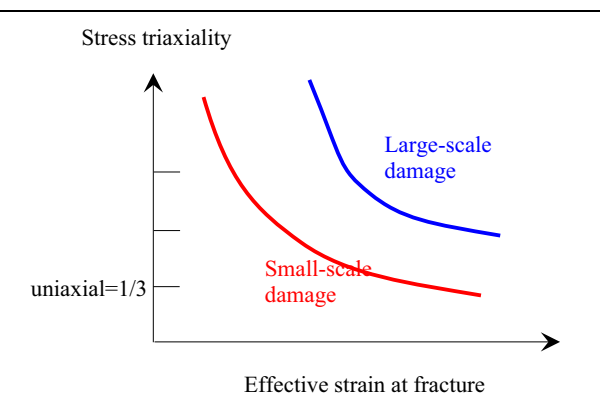


Fig. 4. The dependence of fracture strain on stress triaxiality in notched bars, schematically showing the numerical results from Needleman and Tvergaard <sup>10</sup> Similar to the SSB–LSB competition, the extent of the damage zone as compared with the notch root radius or other geometric features can significantly change the failure strain.

failure resembles the bridged crack in mode II, and the cavitation failure in BMGs shares the essential stress triaxiality dependence of the GTN model. However, these two processes are much more complicated than the simple models shown in Figs. 1 and 3; For example, multiple shear bands can emanate from the notches, and the pressure dependence of shear band initiation has several origins on the atomistic scale, which is still under debate even after extensive atomistic simulations. We first review several sets of experiments, then compare various interpretations in literature, but based rather on our perspective through the interpretations shown in Figs. 1, 2, 3 and 4.

# NOTCH BRITTLENESS VERSUS INVERSE NOTCH EFFECTS IN BMGS

For a notched bar with initial diameter W, reduced diameter L, and notch radius a, similar to the drawing in Fig. 1, the Bridgman solution relates the stress triaxiality T (i.e., the ratio of the mean stress to the effective Mises stress) to the geometric features of the notch by

$$T = \frac{\sigma_{\rm m}}{\sigma_{\rm e}} = \frac{1}{3} + \ln\left(\frac{L}{4a} + 1\right),\tag{5}$$

which is based on the fully plastic analysis from a Mises solid. Assembling a number of literature works <sup>11–19</sup> and following the representation in Pan et al. <sup>16,17</sup> Figure 5 shows distinctive findings, including notch sensitivity (i.e., notches will reduce the strength, so-called notch brittleness) and inverse notch effect (i.e., notches will increase the strength, and the failure mode changes from shear bands to cavitation).

In one of the earliest experimental works, Flores and Dauskardt<sup>12</sup> found the classic notch brittleness in BMGs (i.e., the downward trend in Fig. 4). The fracture strength in their Zr-based BMGs reduced from 2.4 GPa to 1.5 GPa with increase of the stress

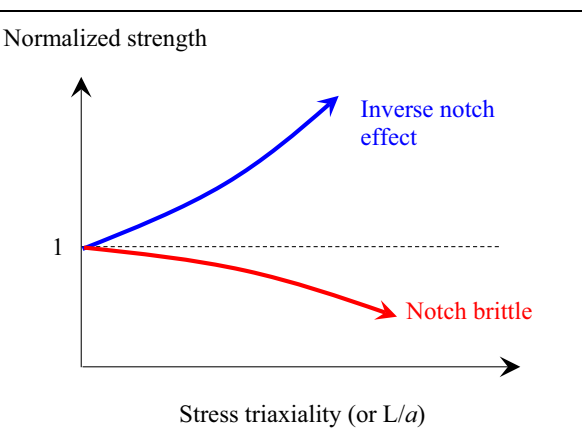


Fig. 5. Notch sensitivity in BMGs, showing both the conventional notch brittleness and the inverse notch effect, schematically showing the experimental results from Pan et al. 16,17.

880 Zhao and Gao

triaxiality. As they did not find cavitation failure, the mechanism in Fig. 3 is not applicable. Their interpretation invokes a modification to Spaepen's free volume model.

In Spaepen's model,<sup>20,21</sup> the plastic strain rate is related to the stress-biased jumps of atoms, which is facilitated by the excess free volume,

$$\frac{\partial \varepsilon_{ij}^{p}}{\partial t} = v \exp\left(-\frac{\Delta G^{m}}{k_{\rm B}T}\right) \exp\left(-\frac{\alpha v^{*}}{v_{\rm f}}\right) \sinh\left(\frac{\sigma_{\rm e}\Omega}{2k_{\rm B}T}\right) \frac{s_{ij}}{\sigma_{\rm e}},\tag{6}$$

where v is the vibration frequency,  $\Delta G^m$  is the intrinsic activation barrier for an atom to jump into a nearby vacancy,  $k_{\rm B}$  is the Boltzmann constant,  $v_{\rm f}$  is the free volume,  $\sigma_{\rm e}$  is the Mises stress, and  $s_{ij}$  is the deviatoric stress tensor that generalizes Spaepen's original one-dimensional model to a multiaxial stress state. The free volume is treated as a state variable in the constitutive model, and its evolution is specified by

$$\begin{split} \frac{\partial v_f}{\partial t} &= v^* v \exp\left(-\frac{\Delta G^m}{k_{\rm B}T}\right) \exp\left(-\frac{\alpha v^*}{v_{\rm f}}\right) \\ &\times \left\{\frac{2\alpha k_{\rm B}T}{v_f C_{\rm eff}} \left[\cosh\left(\frac{\sigma_{\rm e}\Omega}{2k_{\rm B}T}\right) - 1\right] - \frac{1}{n_{\rm D}}\right\}, \end{split} \tag{7}$$

in which the creation of free volume is treated as an Eshelby inclusion problem with effective modulus  $C_{\rm eff}$ , and the annihilation of free volume is via a diffusional process after a few jumps ( $n_{\rm D}$  usually being taken as an integer of 3 to 5). Neither Eqs. 6 nor 7 depends on the hydrostatic stress, so the shear bands are not affected by the high stress triaxiality in notched samples.

Flores and Dauskardt<sup>12</sup> introduced a modification to Eq. 7 by considering the hydrostatic expansion of free volume,

$$v_{\rm f,initial} = v_{\rm f,0} \left( 1 + \frac{\sigma_{\rm m}}{R} \right),$$
 (8)

where *B* is the bulk modulus. As the mean stress depends on the notch geometric factor, L/a, through Eq. 5, the increase of initial free volume in Eq. 8 promotes the occurrence of strain localization in the constitutive model in Eqs. 6 and 7. While the prediction agrees nicely with their experimental findings, this approach suffers the shortcoming that these constitutive parameters and the free volume are not easily measurable and also cannot be calibrated from atomistic simulations. Regardless of the atomistic details, the way of introducing the mean stress into the constative law should be constrained by the tensor mechanics and thermodynamics for dissipative processes, which have been extensively discussed by Chen et al.<sup>22,23</sup> These works specify the general forms for incorporating the mean stress into the yield surface and flow direction, and can be further generalized to include thermal transport.<sup>3</sup>

To rationalize their finding of inverse notch effects, Pan et al. 15-17 invoked two mechanisms, viz. (1) competition between the cavitation strength,  $\sigma_{\rm c}$ , and shear band failure strength,  $\sigma_{\rm s}$ , and (2) relaxation of free volume by the mean stress, which delays shear band failure. The former mechanism appears to resemble the GTN model in Fig. 3, but the micromechanical processes are radically different, since the void growth in the GTN model is through Mises plastic deformation. Additionally, experimental validation of homogeneous cavity nucleation in BMGs is extremely challenging, and only heterogeneous nucleation in shear bands has been observed. Nevertheless, an upper bound on the ratio  $\sigma_{\rm c}/\sigma_{\rm s}$  has been derived by Wei.<sup>24</sup> The latter mechanism involves a very different modification to the Spaepen model than that shown in Eq. 8. The diffusional process, as described by the term with  $n_{\rm D}$ , is now replaced by the stress-biased diffusion coefficient, given by

$$\left. \frac{\partial v_{\rm f}}{\mathrm{d}t} \right|_{\rm annihilation} \propto \exp \left( -\frac{\Delta G^m - \sigma_{\rm m} V}{k_{\rm B} T} \right) \eqno(9)$$

where V is the activation volume. Consequently, notches introduce a large mean stress, which facilitates free volume annihilation, so that the shear band initiation obtained from the constitutive model in Eqs. 6 and 7 will be delayed. This is opposite to the prediction of Eq. 8.

The models presented above in Eqs. 8 and 9 lack predictive capability, because the expected mechanisms are very difficult to verify or calibrate using atomistic studies. Recent work by Lei et al. 25 combined experimental studies and continuum and atomistic simulations, quantitatively determining for the first time the competition between shear failure and normal mode fracture. This paves the way for further development of constitutive studies of this transition. Specifically, a constitutive law needs to couple the evolution of one or many state variables, describing structural order (such as free volume) and extent of damage (such as void fraction), which will predict the simultaneous processes of strain localization and damage.

# SYNERGISTIC EFFECTS FROM VARIOUS MECHANISMS

As the deformation behavior in BMGs is governed by strain localization into shear bands, we need to incorporate two more mechanisms. First, under uniaxial loading conditions, BMGs fail catastrophically immediately after shear band initiation because of the lack of geometric constraints of the major shear band. Referring to Fig. 6, if the notched segment is too tall, the entire sample will fail, as in uniaxial tests of plates or bars. On the other hand, if the height of the notched segment is low, multiple shear bands will emanate from the notch roots, thus reducing the effective shear strain on each shear

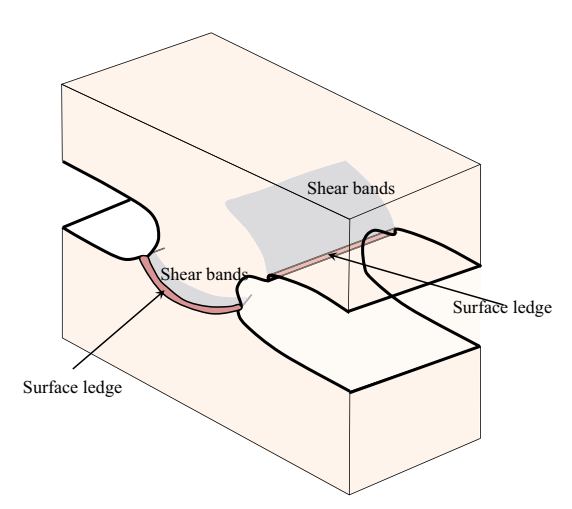


Fig. 6. In addition to the role of stress triaxiality in shear band initiation and cavitation failure, shear band arrangements from the notch roots also contribute to the BMG notch effect. Reprinted from Ref. 18 under Creative Commons Attribution 4.0 International License.

band and delaying the evolution from shear banding to shear failure. The extent of these shear bands can be roughly estimated from the plastic zone size, calculated by using the Mises or Drucker-Prager plasticity model. Large-scale yielding is preferable, since the plastic zone can then grow away from notches, albeit limited by other boundary conditions. Second, the transition from shear bands to cavitation failure in Pan et al. 16,17 should not be a sharp one. Shear band initiation certainly relaxes the stress concentration and thus delays the complete transition to cavitation failure. Under these circumstances, the weak zones (which are shear bands in our case) will relieve the stress concentration along the cavitation plane and thus delay this ductile fracture, as noticed in the competition between decohesion and dislocation emission<sup>26</sup> and in continuum plasticity simulations.<sup>27</sup> The same idea has been used in composite mechanics. In Fig. 1, one can introduce various weak zones near the notches or cracks, so that LSB is more likely to occur and the composite will have higher toughness due to the additional energy dissipation into these weak zones.

# UNIFIED PERSPECTIVE ON NOTCH EFFECTS

Summarizing the above discussions on notch experiments in composites, conventional metallic materials, and BMGs, the following unified perspective can be developed:

 Notch brittleness versus notch ductileness can be tuned via the crack-bridging characteristics, as in composite mechanics. SSB makes it brittle, while LSB makes it ductile. For BMGs, this can be done by:

- (a) Emanating multiple shear bands from notch roots and extending these shear bands away from notches
- (b) Identifying the relevant strength and separation parameters, i.e.,  $\sigma_0$  and  $\delta_0$ , upon treating the cavitation fracture as a cohesive interface model
- Notch brittleness versus notch ductileness can be tuned from the extent of damage zone as in the GTN model for conventional metals and alloys. SSY or SSD makes it brittle, while LSY or LSD makes it ductile. For BMGs, this can be done by
  - (a) Estimating the plastic zone from a continuum Mises or Drucker–Prager model
  - (b) Developing a GTN-type void model for BMGs (which appears to be feasible from recent atomistic simulations, but with confusion arising from the locations of void nucleation)
- 3. The notch sensitivity of BMGs depends on a number of atomistic processes, on which consensus has not been reached, including:
  - (a) The role of stress triaxiality in the flow equation (for  $\dot{\varepsilon}_{ij}^p$ ) and evolution equation (for the state variable, e.g., free volume)
  - (b) The role of stress triaxiality in the growth of cavities.
- 4. The notch sensitivity of BMGs depends on how microscopically shear bands are arranged, leading to:
  - (a) Stress redistribution and strain reduction on multiple shear bands
  - (b) The delay of cohesive fracture or cavitation from the shear bands
- 5. The failure process in BMGs should be modeled based on some microscopic processes of damage initiation and evolution, while unit events such as void growth should be simulated using atomistic models. This remains elusive, but BMG notch experiments can provide both insight and validation examples.

### **ACKNOWLEDGEMENTS**

Y.Z. was supported by the China Scholarship Council (No. 201808625027), National Natural Science Foundation of China (Grant No. 51661017), and Outstanding Youth Funds of Gansu Province of China (Grant No. 17JR5RA108). Y.G. acknowledges support from the US National Science Foundation (DMR 1809640).

### REFERENCES

- J.W. Rudnicki and J.R. Rice, J. Mech. Phys. Solids 23, 371 (1975).
- Y.F. Gao, L. Wang, H. Bei, and T.G. Nieh, Acta Mater. 59, 4159 (2011).

882 Zhao and Gao

- X. Xie, Y.C. Lo, Y. Tong, J. Qiao, G. Wang, S. Ogata, H. Qi, K.A. Dahmen, Y.F. Gao, and P.K. Liaw, J. Mech. Phys. Solids 124, 634 (2019).
- 4. G. Bao and Z. Suo, Appl. Mech. Rev. 45, 355 (1992).
- J.W. Hutchionson and A.G. Evans, Acta Mater. 48, 125 (2000).
- 6. V. Tvergaard, Adv. Appl. Mech. 27, 83 (1990).
- 7. A. Needleman, Proc. IUTAM 10, 221 (2014).
- 8. B.H. Ji and H.J. Gao, J. Mech. Phys. Solids 52, 1963 (2004).
- A.A. Benzerga and J.B. LeBlond, Adv. Appl. Mech. 44, 169 (2010).
- A. Needleman and V. Tvergaard, *J. Mech. Phys. Solids* 32, 461 (1984).
- K.M. Flores and R.H. Dauskardt, J. Mater. Res. 14, 638 (1999)
- 12. K.M. Flores and R.H. Dauskardt, *Acta Mater.* 49, 2527 (2001).
- W. Chen, Z. Liu, H.M. Robinson, and J. Schroers, *Acta Mater.* 73, 259 (2014).
- W. Chen, Z. Liu, J. Ketkaew, R.M.O. Mota, S.H. Kim, M. Power, W. Samela, and J. Schroers, Acta Mater. 107, 220 (2016)
- Z.T. Wang, J. Pan, Y. Li, and C.A. Schuh, *Phys. Rev. Lett.* 111, 135504 (2013).

- J. Pan, H.F. Zhou, Z.T. Wang, Y. Li, and H.J. Gao, J. Mech. Phys. Solids 84, 85 (2015).
- J. Pan, Y.X. Wang, Q. Guo, D. Zhang, A.L. Greer, and Y. Li, Nat. Commun. 9, 560 (2018).
- W.D. Li, Y.F. Gao, and H. Bei, Sci. Rep. 6, 34878 (2016).
- 19. W.D. Li, H. Bei, and Y.F. Gao, Intermetallics 79, 12 (2016).
- 20. F. Spaepen, Acta Metall. 25, 407 (1977).
- Y.F. Gao, Modell. Simul. Mater. Sci. Eng. 14, 1329 (2006).
- Y. Chen, M.Q. Jiang, Y.J. Wei, and L.H. Dai, *Phil. Mag.* 91, 4536 (2011).
- 23. Y. Chen and L.H. Dai, Int. J. Plast. 77, 54 (2016).
- 24. Y.J. Wei, Theoret. Appl. Frac. Mech. 71, 76 (2014).
- X.Q. Lei, C.L. Li, X.H. Shi, X.H. Xu, and Y.J. Wei, Sci. Rep. 5, 10537 (2015).
- 26. V. Shastry and P.M. Anderson, Phil. Mag. 75, 771 (1997).
- I. Singh, T.F. Guo, P. Murali, R. Narasimhan, Y.W. Zhang, and H.J. Gao, J. Mech. Phys. Solids 61, 1047 (2013).

**Publisher's Note** Springer Nature remains neutral with regard to jurisdictional claims in published maps and institutional affiliations.